Hindawi
Geofluids
Volume 2022, Article ID 5224154, 11 pages
https://doi.org/10.1155/2022/5224154

Research Article

Experimental Study on Heat Transfer Process Optimization of Heat Storage Wall of the Heat Pump in Tunnel Surrounding Rock in the Cold Region

Yafei Li,[1] **Dianwei Qi**,[1] **Hongchao Yan**,[2] **and Jiaqi Zhang**[1]

[1]*College of Civil Engineering and Architecture Xinjiang University, Urumqi 830017, China*
[2]*School of Business Xinjiang University, Urumqi 830091, China*

Correspondence should be addressed to Dianwei Qi; qidianwei@xju.edu.cn

Received 25 July 2022; Revised 24 August 2022; Accepted 5 September 2022; Published 27 September 2022

Academic Editor: Dongjiang Pan

For tunnels in cold or serious cold areas, the problem of leaking in the spring thawing period is very frequent, which will cause various tunnel diseases due to freezing. By using the surrounding rock geothermal energy in the tunnel project, especially the tunnel project below the permafrost layer, the cold area tunnel heat pump system is able to improve the overall heating energy efficiency as the side temperature regarding the heat pump evaporation increases, that furtherly serves the surrounding supporting building facilities. Inspired by this system and the active and passive coupling building technology, a heat recovery type of heat storage wall model is proposed in this research. By describing the heat transfer process regarding the heat recovery type of heat storage wall and carrying out the experimental research, its feasibility and effectiveness are verified. The results show that when the outdoor ambient temperature in Urumqi is −7~−15°C and the instantaneous total solar radiation reaches the range of 0~1108 W/m^2, this kind of wall can create hot wall-near air whose temperature is 11.89°C higher than the ambient temperature for providing a high-quality air heat source for the air source heat pump when the temperature is low, thereby significantly improving the air source heat pump heating system efficiency. Without the photovoltaic and photothermal equipment, the heat recovery type of heat storage wall can make the utilization rate of solar energy reach 13% to 20%, even up to 36%.

1. Introduction

Due to the worsening world energy crisis, the use of renewable energy has drawn much attention, and its application in tunnel engineering in cold regions has emerged in an endless stream. Brandl [1] and Yuan et al. [2] applied ground source heat pump (GSHP) to tunnels in cold areas and improved the energy efficiency of GSHP by absorbing the geothermal energy of surrounding rocks, so as to serve the heating of tunnels and nearby buildings. Some scholars [3, 4] even found that the subway tunnel structure can obtain an annual average heat of 175 MWh and an annual average refrigeration capacity of 437 MWh.

The heat storage wall constitutes the passive solar house and has simple structure, convenient maintenance, and high thermal stability, and it is widely used in northern villages where solar energy resource is abundant. This kind of wall first appeared in the study of the group of Professor Felix Trombe, who is the director of the French Solar Energy Laboratory, also called the Trombe wall. In recent years, with continuous research on the heat storage wall, its application field is becoming more widespread. Rabani and Kalantar [5] put forward a new heat storage wall capable of receiving solar radiation in three directions, increasing the indoor space as well as reducing the implementation cost; the results show that this new heat storage wall has a good heat storage effect and thermal efficiency. By simplifying the physical model of the heat storage wall, Chen et al. [6] used a combination method of numerical simulation and in situ measurement for studying the dynamic heat storage as well as heating characteristics exhibited by the wall when the thermal insulation structures are different. Elghamry and

Hassan [7] studied through experimentation of the heat storage wall combined with geothermal energy, solar energy, etc., and it is proved that this combination system can provide the best heating and ventilation performance. Shen [8] performed a numerical simulation study about the heat distribution law of a heating room with heat storage walls, finding that the heating capacity can be improved as the heat storage wall height and width increase. Liu et al. [9] introduced the Trombe wall to the cavity building system using a numerical simulation method and found that the partitioned Trombe wall cavity building system has more advantages than the connected Trombe wall cavity building system. Mehran Rabani and Mehrdad Rabani [10] added metal fins to the Trombe wall channel, and the experimental results show that fins can indeed strengthen the energy storage; among three kinds of fins, the effect of copper fins is the best. Sun and Wang [11] conducted a numerical simulation study about the phase change heat storage wall performance in the Qinghai-Tibet Plateau, finding the positive effect exerted by phase change materials on its heating stability. Lou et al. [12] gave a design scheme for strengthening the thermal insulation performance of rooms with Trombe walls at night through simulation and experimental verification. Li et al. [13] found that the Trombe wall height change can effectively affect the flow channel wind speed.

With the renewable energy utilization being promoted, the research of heat pump system spreads out from various levels. Many scholars [14–18] put forward the parallel system of multienergy complementarity, which improves the stability of heating system by combining heat pump system and solar system in parallel. Some scholars [19–21] have also proposed a series system with complementary multienergy, connecting the heat pump system with the solar air collector in series to improve the overall heating energy efficiency by increasing the heat pump evaporation temperature.

In summary, the current research on heat storage walls mainly focuses on daytime air heat utilization, convective heat transfer improvement, and dynamic heat transfer characteristics. However, there is limited research on how to make more efficient use of daytime heat storage and convection heat transfer of heat storage walls as well as the linkage operation with active energy supply heat pump equipment for improving the wall heat dissipation performance. Inspired by the idea of combining the heat pump system with tunnel engineering for enhancing the energy efficiency regarding the heat pump and better serving the infrastructure facilities around the tunnel, the active and passive building technology are innovatively incorporated with them in this paper to establish and propose a coupling system of the heat recovery type of heat storage wall and air source heat pump. We propose a heat recovery type of heat storage wall structure, in which a transparent air space layer is added to the outside of the existing wall to utilize two parts of the heat in this air space layer, part of the heat is lost by heat transfer, and the other part is obtained by the outer surface of the wall with high absorption rate absorbing the heat of solar radiation. These two parts of heat are exchanged with the interlayer air through convection so that the outdoor air at ambient temperature becomes the source of low-temperature air source heat pump after being preheated by the interlayer; then, this heat pump improves the overall energy efficiency of the building by recovering dissipated wall heat and solar radiation heat.

2. Physical Model

The heat recovery type of heat storage wall is shown in Figure 1, which consists of the standard energy-saving structure wall, air interlayer, and transparent cover plate. The air with outdoor ambient temperature enters through the orifice plate at the lower part of the air interlayer and is confluent from the top orifice plate and then sent to the air suction port of the air source heat pump evaporator.

The air interlayer is 200 mm thick, and the plane dimension of the heat storage wall is 1500 mm in width and 2000 mm in height. Three orifices are opened on the wall below the air interlayer to let the outdoor air enter the air interlayer, and the size of the orifice is 15 cm ×4 cm. The size of the orifice at the centre above the air interlayer is the same as that of the fan duct φ16 cm. Table 1 lists the physical parameters exhibited by each enclosure wall layer and the heat recovery type of heat storage wall is shown in Figure 2.

The solar radiation absorption coefficient of the outer surface of wall $\alpha_{\text{wall}} = 0.75$.

3. Methodology

The most significant difference between such heat storage wall and the ordinary heat storage wall is the air flow state regarding the interlayer. The heat exchange on the ordinary heat storage wall surface is natural convection; the air in the interlayer of the heat recovery type of heat storage wall is forced to occur convection. The heat transfer process of the heat recovery type of heat storage wall includes three parts: transparent cover plate, air interlayer, and heavy wall structure [22], and their heat transfer and heat exchange processes are displayed in Figure 3.

The heat exchange between the transparent cover plate and the surrounding environment includes absorbing solar radiation, heat exchange through natural convection with outdoor air, radiation heat exchange with the sky, and heat exchange through forced convection with interlayer air as well as radiation heat exchange with the outer wall surface [23]. Because the transparent cover plate is very thin, we can basically confirm that the temperature in the thickness direction, that is, the y-direction, is the same. Affected by the temperature gradient distribution at the height of the air in the interlayer, how the temperature is distributed in the transparent cover plate is the one-dimensional heat transfer in the height direction, i.e., the x-direction; regarding the transparent cover plate, equations (1)–(8) show the energy balance equation [24–26].

$$\begin{aligned}\rho C_P D_g \frac{\partial T_P}{\partial t} = {} & \lambda_x D_g \frac{\partial^2 T_p}{\partial x^2} + \alpha_P G + h_{r,\text{amb}}\left(T_{\text{sky}} - T_p\right) \\ & + h_{c,\text{amb}}\left(T_{\text{out}} - T_p\right) + h_{r,i}\left(T_{wo} - T_p\right) \\ & + h_{c,ch}\left(T_a - T_p\right).\end{aligned} \tag{1}$$

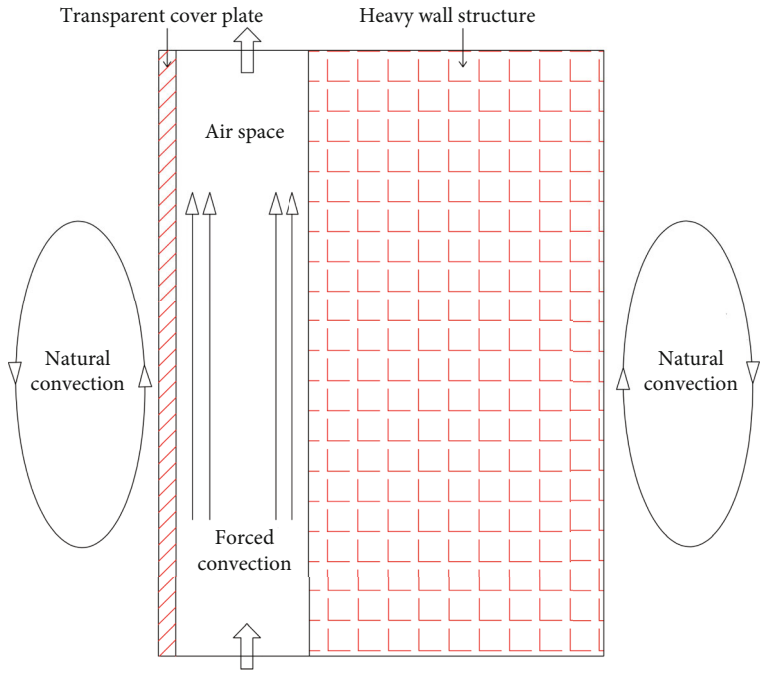

Figure 1: Schematic diagram of heat recovery type of heat storage wall.

Table 1: Physical property parameters of each layer of the enclosure wall.

Material type	Thickness (mm)	Conductivity coefficient W/(m·K)	Heat storage coefficient W/(m^2·K)	Heat resistance (m^2·K)/W	Thermal inertia index $D = R \cdot S$
Cement mortar	10	0.930	11.37	0.011	0.12
Aerated concrete block	200	0.190	2.81	0.842	2.96
Cement mortar	21	0.930	11.37	0.023	0.26
Vertical wire rock wool	100	0.045	0.75	1.852	1.67

Figure 2: Physical diagram of heat recovery type of heat storage wall.

In the equation, ρ is the transparent cover plate density, kg/m^3; C_p is the specific heat capacity regarding the transparent cover plate, J/(kg·K); D_g is the transparent cover plate thickness, m; T_p is the transparent cover plate temperature, K; λ_x is the thermal conductivity regarding the transparent cover plate in the x-direction, W/(m·K); α_P is the solar radiation absorptivity regarding the transparent cover plate; G is the radiation intensity of solar vertically incident on the transparent cover plate surface, W/m^2; $h_{r,\mathrm{amb}}$ is the coefficient of radiation heat transfer between transparent cover plate and sky, W/(m^2·K); T_{sky} is the sky temperature, K; $h_{c,\mathrm{amb}}$ is the natural convection heat transfer coefficient between transparent cover plate and the outdoor air, W/(m^2·K); T_{out} is the ambient air temperature, K; $h_{r,i}$ is the coefficient of radiation heat transfer between transparent cover plate and heavy outer wall surface, W/(m^2 K); T_{wo} is the heavy outer wall surface temperature, K; $h_{c,ch}$ is the forced convection heat transfer coefficient between the transparent cover plate and the interlayer air, W/(m^2·K); and T_a is the interlayer air temperature, K.

$$h_{r,\mathrm{amb}} = \sigma\varepsilon_o\left(T_p{}^2 + T_{\mathrm{sky}}{}^2\right)\left(T_p + T_{\mathrm{sky}}\right), \tag{2}$$

$$h_{r,i} = \frac{\sigma\left(T_p{}^2 + T_{wo}{}^2\right)\left(T_p + T_{wo}\right)}{\left(1/\varepsilon_i + 1/\varepsilon_{wo} - 1\right)}, \tag{3}$$

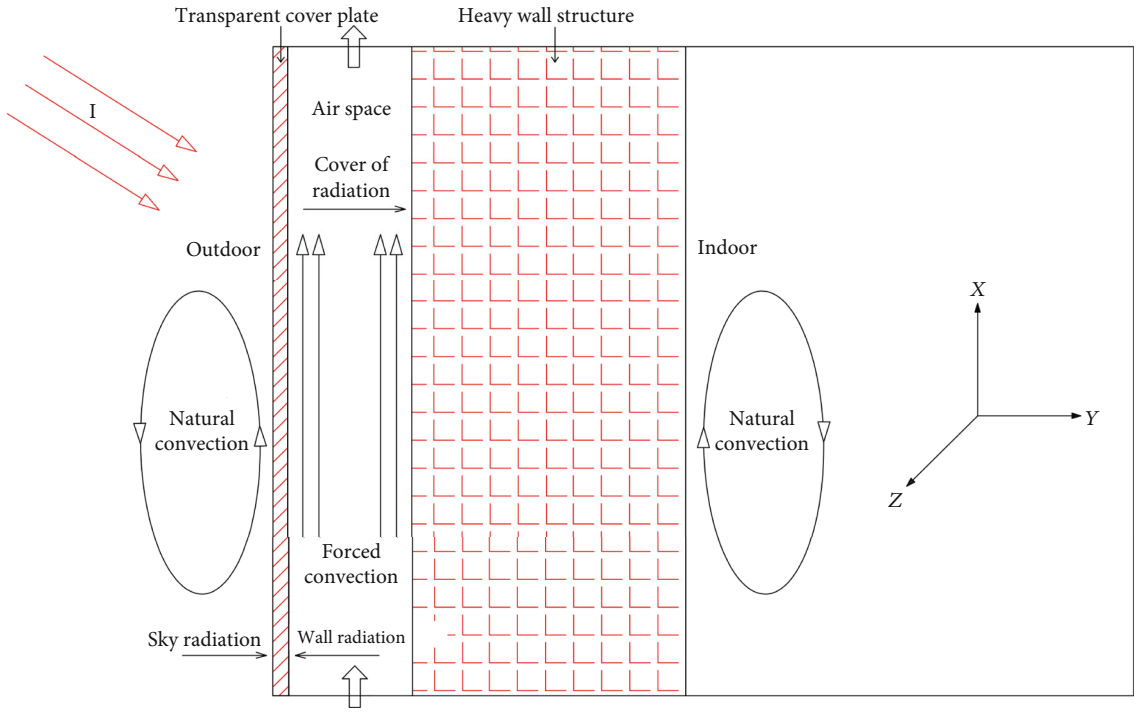

Figure 3: Schematic diagram of heat transfer and exchange process of heat storage wall.

where σ is the Stefan-Boltzmann constant, $5.67 \times 10\text{-}8\ \mathrm{W/(m^2{\cdot}K^4)}$; ε_o is the emissivity outside the transparent cover plate; ε_i is the emissivity inside the transparent cover plate; and ε_{wo} is the outer wall surface emissivity.

Sky temperature:

$$T_{\mathrm{sky}} = 0.0552 T_{\mathrm{out}}{}^{1.5}. \tag{4}$$

Calculation of convection heat transfer coefficient:

$$h_{c,amb} = 2.8 + 3.0v, \tag{5}$$

$$h_{c,ch} = \frac{N_{u,X}\lambda_{\mathrm{a}}}{X}, \tag{6}$$

$$N_{u,X} = (0.0158 R_{e,X})^{0.8}, \tag{7}$$

$$R_{e,X} = \frac{\mathrm{VX}}{\upsilon}, \tag{8}$$

where v is outdoor wind speed, m/s; λ_a is the interlayer air thermal conductivity, W/(m·K); V is the air speed in the interlayer, m/s; and υ is the interlayer air movement viscosity, $\mathrm{m^2/s}$.

The interlayer air and the surrounding environment heat exchange includes the forced convection heat exchange with the transparent cover plate and the heavy outer wall surface, the corresponding energy balance equation is shown.

$$\rho_a C_{p,a} D \frac{\partial T_a}{\partial t} = h_{c,ch}\left(T_p - T_a\right) + h_{c,wo}\left(T_{wo} - T_{\mathrm{a}}\right) - \mathrm{DV}\rho_a C_{\mathrm{p,a}} \frac{\partial T_a}{\partial x}, \tag{9}$$

where ρ_a is the interlayer air density, $\mathrm{kg/m^3}$; $C_{p,a}$ is the specific heat capacity regarding the interlayer air, J/(kg·K); D is the air interlayer thickness, m; and $h_{c,wo}$ is the forced convection heat transfer coefficient between the interlayer air and the heavy outer wall surface, $\mathrm{W/(m^2{\cdot}K)}$; the meanings of other parameters are the same as before.

The heavy wall and the environment heat exchange includes the absorbed solar radiation, the radiation heat exchange with the transparent cover plate, the forced convection heat exchange with the interlayer air, and the natural convection heat exchange with the indoor air. Here, the solar radiation passes through the transparent cover plate to the outer surface of the wall and is then reflected then ignored as the transparent cover plate exhibits high transmittance and the outer wall surface has low reflectivity. Assuming that the distribution of indoor temperature is uniform and the difference in temperature between the inner wall surfaces is not obvious, the radiation heat transfer between indoor side walls can also be ignored [27]. The heat conduction of the heavy wall structure is mainly along the thickness direction and is one-dimensional heat transfer along the thickness direction, that is, the y-direction [28–30]. Equation (10) gives the energy balance equation regarding the heavy wall structure.

$$\rho_{\mathrm{wall}} C_{\mathrm{wall}} D_{\mathrm{w}} \frac{\partial T}{\partial t} = \lambda_{\mathrm{wall}} D_{\mathrm{w}} \frac{\partial^2 T}{\partial y^2} + G\tau\alpha_{\mathrm{wall}} + h_{r,wo}\left(T_p - T_{wo}\right) + h_{c,wo}\left(T_a - T_{wo}\right) + h_{c,wi}\left(T_{\mathrm{r}} - T_{wi}\right), \tag{10}$$

where ρ_{wall} is the density of the heavy wall, $\mathrm{kg/m^3}$; C_{wall} is the

heavy wall heat capacity, J/(kg·K); T is the heavy wall temperature, K; λ_{wall} is the heavy wall thermal conductivity, W/(m·K); D_w is the heavy wall thickness, m; τ is the solar radiation transmittance of the transparent cover plate; α_{wall} is the solar radiation absorptivity of the heavy outer wall surface; $h_{r,wo}$ is the radiation heat transfer coefficient between the outer wall surface and the transparent cover plate, W/(m^2·K), $h_{r,wo} = h_{r,i}$; $h_{c,wi}$ is the convective heat transfer coefficient between the inner wall surface and indoor air, W/(m^2·K); T_{wi} is the heavy wall internal surface temperature, K; and T_r is the indoor air temperature, K; the meanings of other parameters are the same as before.

4. Experiment Results

For exploring the heat transfer characteristics exhibited by the heat recovery type of heat storage wall, it is necessary to arrange measuring points on the wall and measure related parameters, including solar radiation, temperature, and heat flow. Figure 4 gives the specific measuring point layout. This heat storage wall is built on the southern outside of a heating building, and the indoor temperature of the heating building is constant during the data collection. In this experiment, the wall heat loss measurement is based on the heat flow plate attached to the inner wall surface, which avoids the solar radiation influence when the heat flow plate is arranged on the outdoor side. However, the indoor side heat flow plate will still be affected by indoor personnel's disturbance and the outer door's opening. Therefore, in the analysis of the heat loss of the envelope structure, the extreme peak value can be ignored.

4.1. Analysis of Thermal Work of Heat Recovery Type of Heat Storage Wall. Aiming at analyzing the heat storage wall thermal performance, it is necessary to first study heat consumption per unit area, i.e., the heat loss, measured mainly by connecting the heat flow meter to the heat flow plate arranged inside the ordinary wall and heat storage wall. As found by the research on the thermal performance regarding ordinary heat storage wall, adding a closed air interlayer on the outside of the heavy wall structure can greatly improve its thermal performance and reduce the heat consumption. The heat recovery type of heat storage wall opens up and down holes in the air interlayer and adds a fan to change the flow state of the interlayer air; its thermal performance needs to be further studied through experiments. Figure 5 compares the heat recovery type of heat storage wall and the ordinary wall in terms of the heat flow.

These two kinds of walls present consistent overall changing trend of the heat flow, and the changing trend is mainly affected by the comprehensive impact exerted by the outdoor environmental parameters: air temperature and solar radiation (Figure 5). The average heat flow of the ordinary wall is 18.5 W/㎡, and the average heat flow of the heat recovery type of heat storage wall is 5.9 W/㎡, indicating that the latter wall has a significant improvement effect compared with the former wall regarding the thermal performance, which remarkably decreases the heat dissipation through the wall structure as well as the heating energy consumption regarding the heating room.

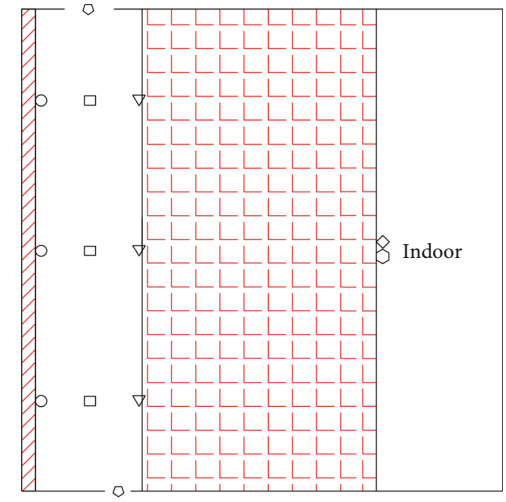

Figure 4: Layout of measuring points.

4.2. Analysis of Energy Efficiency of Heat Recovery Type of Heat Storage Wall

4.2.1. The Inlet and Outlet Air Temperature Difference of the Interlayer. The heat recovery type of heat storage wall is proposed to utilize the high-quality low-temperature air heat source in the air interlayer; therefore, the inlet and outlet air temperature difference of the interlayer significantly affects the evaluation on the storage wall performance. Figure 6 shows the changes in solar radiation as well as the temperature difference in five consecutive days from December 30, 2021 to January 3, 2022.

According to the changing trend of the temperature difference and the instantaneous value of the total solar radiation, during the day, the change of the temperature difference change is consistent with the instantaneous total solar radiation value, showing a positive correlation. In the five consecutive days, the maximum instantaneous total solar radiation value and the maximum temperature difference basically appear at the same moment, indicating the solar radiation immediately affects the temperature difference, and the thermal inertia of the air can basically be ignored. At night, the affecting factors of the temperature difference are the sky radiation and the heat loss of the wall; in the noon period of a sunny day, when the instantaneous total solar radiation value reaches 0~1108 W/㎡, the highest temperature difference can reach 11.89°C. The heated air is sent to the air source heat pump through the fan and

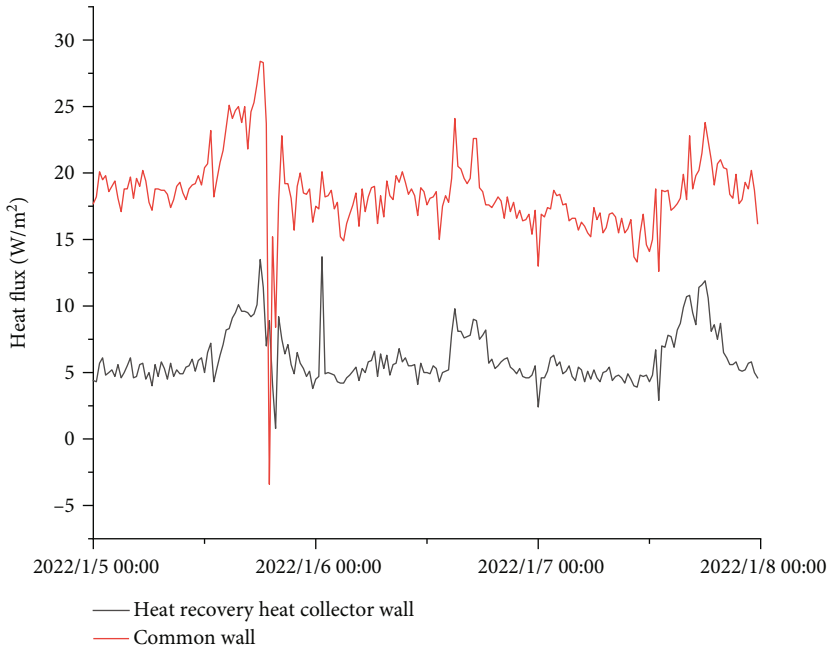

Figure 5: Comparison of wall heat flow.

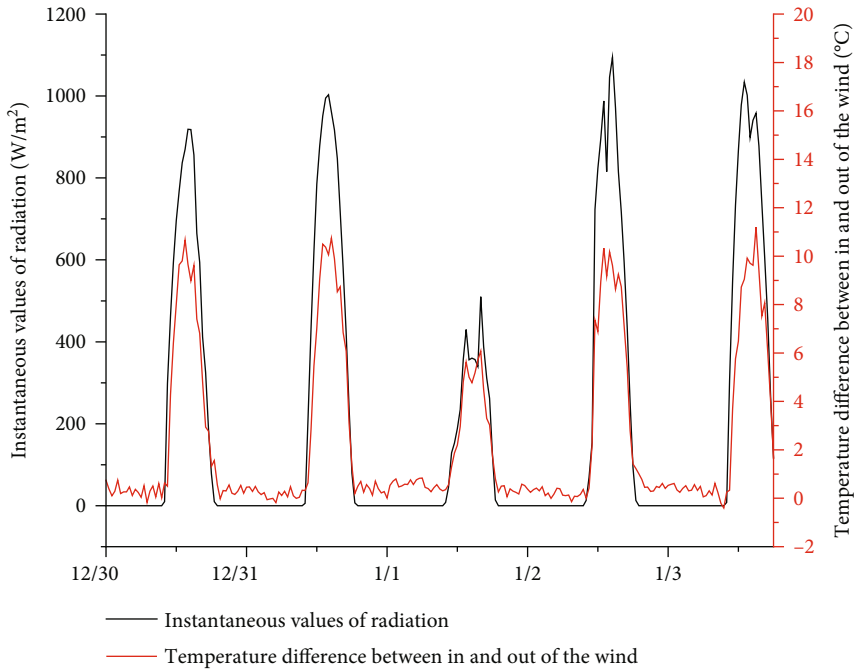

Figure 6: Temperature difference between inlet air and outlet air and solar radiation.

becomes the high-quality low-temperature heat source, which significantly improves the performance coefficient regarding the air source heat pump in the low-temperature environment, thereby enhancing its overall performance of such heat storage wall.

4.2.2. Solar Energy Efficiency Utilization. When analyzing the solar energy utilization, how the wall heat loss affects the interlayer air heat transfer is ignored because the average heat loss of 5.9 W/㎡ is negligible relative to the instantaneous solar radiation.

The solar energy utilization rate in this system is expressed in the following equation:

$$\eta = \frac{c \cdot m \cdot \Delta t}{G \cdot A}. \tag{11}$$

In above equation, η is the solar energy utilization rate; c

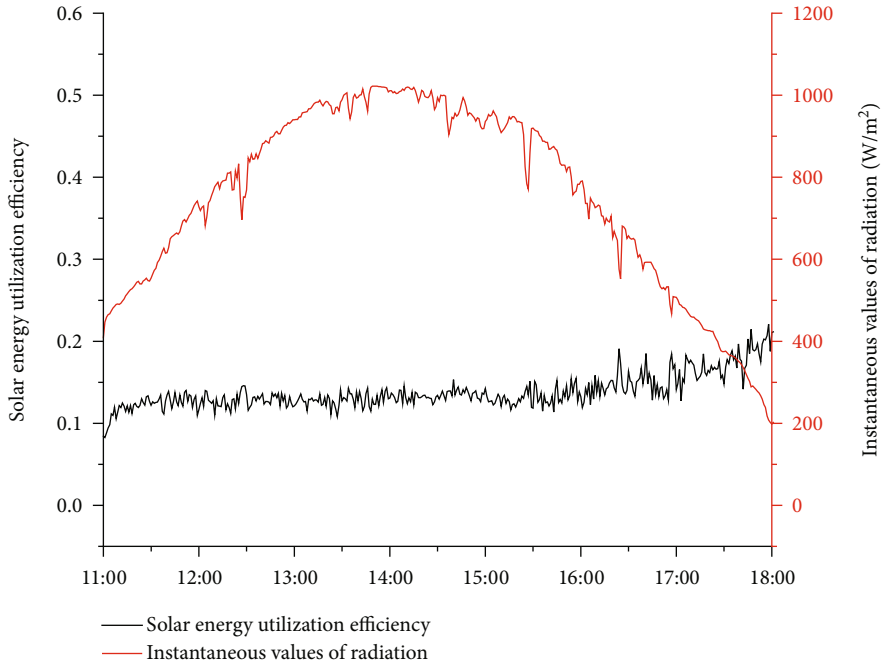

Figure 7: Fan runs at high speed.

is the air constant pressure specific volume, taking 1010 J/(kg·K); m stands for the mass flow rate of the fan suction port, i.e., the interlayer outlet, kg/s; Δt denotes the temperature difference of the interlayer between the inlet and outlet air, K; G denotes the solar radiation intensity vertically incident on the transparent cover plate surface, W/m^2; and A is the light-transmitting part area of the heat storage wall, m^2.

Mass flow at the interlayer air outlet:

$$m = \rho v. \tag{12}$$

In the equation, v is the outlet volume flow, i.e., the fan volume flow, m^3/s; ρ is the outlet air density, kg/m^3.

The correction for air density only takes into account the temperature correction:

$$\rho = \rho_0 \cdot \frac{273}{273 + t_{\text{out}}}, \tag{13}$$

where $\rho_0 = 1.293\,\text{kg/m}^3$ and t_{out} represents the outlet air temperature of the interlayer, ˚C.

Considering that the solar energy utilization rate is meaningful only when there is solar radiation, the data when the fan runs at high and low speeds from 11 : 00-18 : 00 are taken for comparison; Figures 7 and 8 display the results.

Intuitively, when the fan runs at high speed, the solar energy utilization rate is maintained at about 0.13 before 16 : 00 and increases slightly after 16 : 00; when the fan runs at a low speed, the same changing law is shown, and the solar energy utilization rate remained at around 0.2 before 16 : 00, with a maximum of 0.36. It is analyzed that compared with the situation when the fan runs at high speed, the average solar energy utilization rate when the fan runs at a low speed is 0.07 higher; this is, because the interlayer air and the surrounding environment heat exchange are more sufficient. After 16 : 00, no matter whether the fan runs at high or low speed, the solar energy utilization rate has a slight upward trend because the dissipated heat from the heat storage wall has become nonnegligible compared with the solar radiation during this period. Solar energy utilization is already an inaccurate result; Figure 9 shows details.

After 16 : 00, the instantaneous solar radiation value drops suddenly, and the wall dissipated heat increases; the solar energy utilization rate will be overestimated if the heat loss of the wall is ignored at this time. On the other hand, the changing trend of heat loss of the wall also makes up for how solar radiation in the decline stage affects the overall energy efficiency of the heat recovery type of heat storage wall.

4.3. Analysis of Heat Transfer Characteristics of Heat Recovery Type of Heat Storage Wall. The heat transfer process of this type of heat storage wall is analyzed mainly along the thickness direction; therefore, the outer wall temperature regarding the ordinary wall together with the ambient air temperature are, respectively, taken to compare with the outer wall temperature of such heat storage wall and the surrounding interlayer air temperature. The results are shown in Figures 10 and 11, in which legend (no) represents the ordinary wall, (yes) represents the heat recovery type of heat storage wall.

When the fan is turned off, under the action of heat pressure, the interlayer air of the heat recovery type of heat storage wall is subjected to natural convection heat exchange with the outer wall. When the fan is turned on, the interlayer air of the heat recovery type of heat storage wall occurs forced convection heat transfer with the outer wall affected by fan extraction.

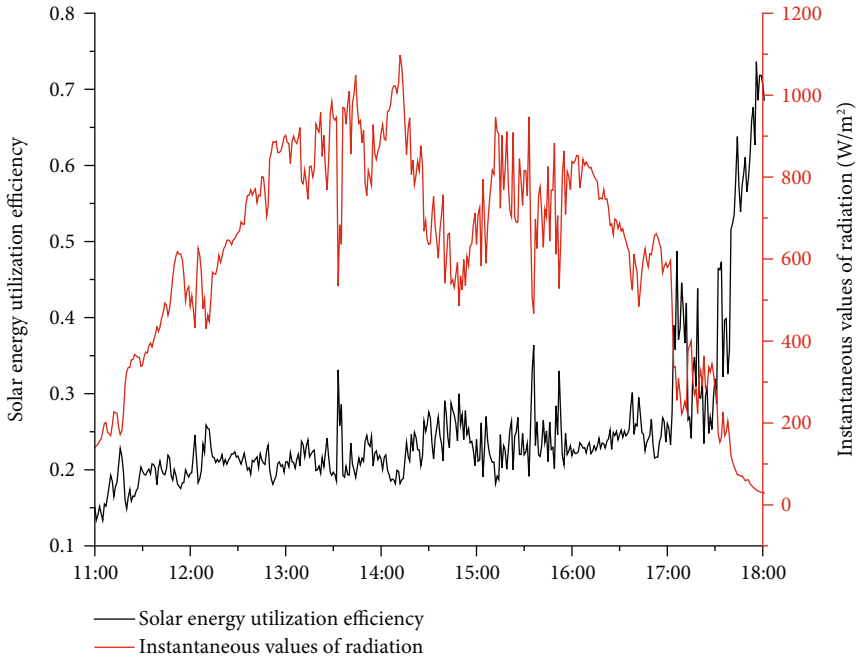

Figure 8: Fan runs at a low speed.

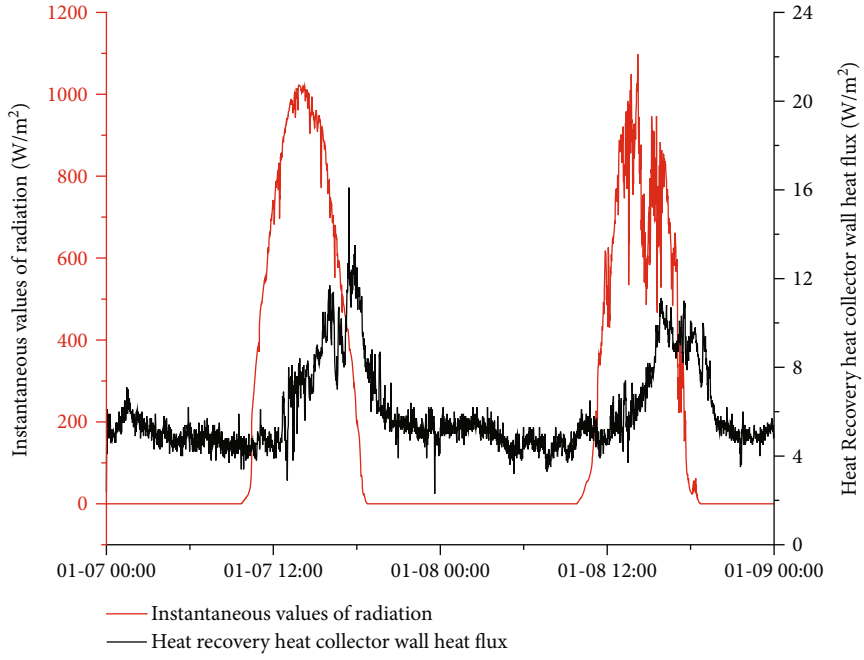

Figure 9: Solar radiation and wall heat flow.

When solar radiation exists during the day, the heat recovery type of heat storage wall exhibited a higher outer wall temperature compared with the ordinary wall when the fan is turned off, and the situation is the opposite when the fan is turned on. This is because when solar radiation exists in the daytime, the outer wall exhibited higher temperature relative to the surrounding air, and heat transfer is conducted through the outer wall with the surrounding air, transferring heat to the surrounding air. As the fan starts to work, the convective heat transfer coefficient between the outer wall of the heat recovery type of heat storage wall is improved, and its heat exchange with the surrounding air becomes more sufficient, making a large amount of heat be continuously taken away and resulting in a lower outer wall temperature of heat storage wall than that of the ordinary wall, which also suggests that the heat recovery type of heat storage wall has a better energy efficiency level when the fan is turned on. At night, under two different working

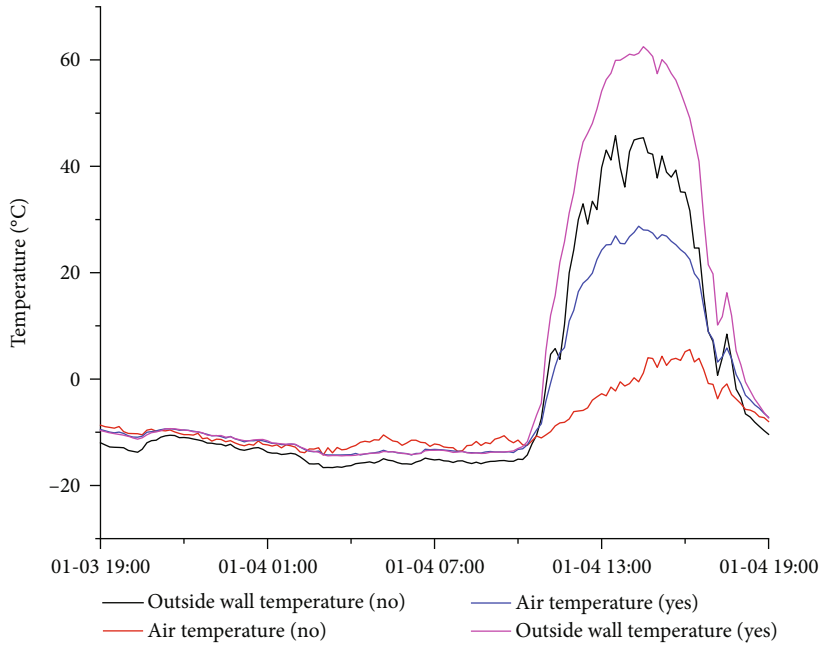

Figure 10: Temperature comparison when the fan stops working.

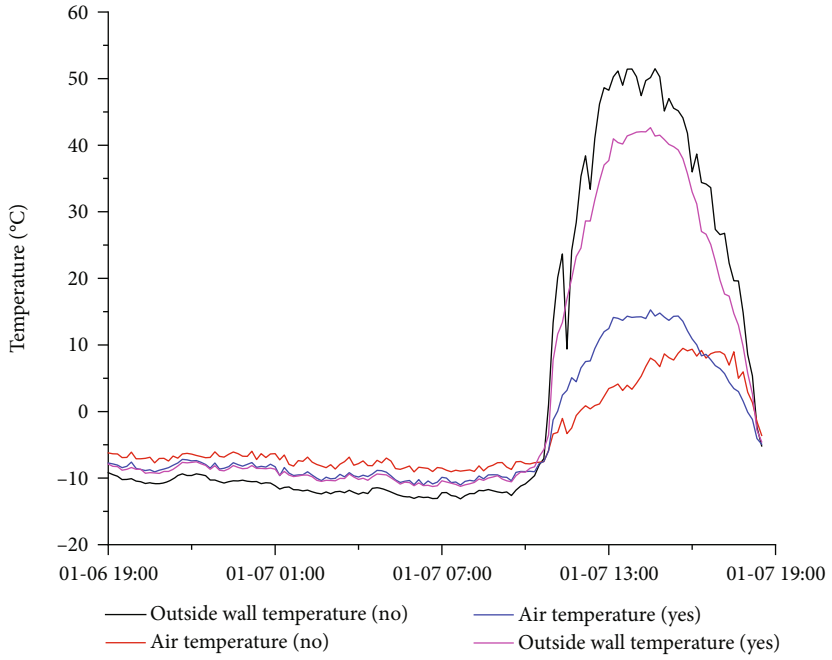

Figure 11: Temperature comparison when the fan runs.

conditions, the heat recovery type of heat storage wall exhibited a higher outer wall temperature relative to the ordinary wall, and the former exhibits a smaller temperature difference relative to the latter. This is because the outer wall surface of the ordinary wall directly receives the sky radiation at night; hence, it exhibits remarkably lower wall surface temperature than the ambient air temperature, while the outer wall surface of the heat recovery type is almost not affected by sky radiation, making the wall surface temperature basically the same as the surrounding air temperature, which also reflects the ability of the heat recovery type of heat storage wall to resist sky radiation at night.

Based on the above analysis of the thermal performance and energy efficiency level of the heat recovery type heat collector wall, it is shown that the system of coupling the passive technology (air source heat pump) and the heat collector wall is completely feasible. In winter, sending the hot air from the air interlayer of the heat collecting wall to

the evaporator side of the air source heat pump will obtain higher energy efficiency value than using the air source heat pump or the heat collecting wall alone.

5. Conclusions

This paper puts forward a new system which combines the passive technology (air source heat pump) and the active energy saving technology (Trombe wall). Through the analysis of the heat transfer process and the experimental results of this new heat recovery wall, some good conclusions are obtained.

(1) The thermal performance of the heat recovery type is significantly improved compared with that of the ordinary wall, which can remarkably lower the dissipated heat through the wall structure and reduce the heating energy consumption of the heating room. This shows that the new thermal recovery wall still retains the excellent thermal performance of the traditional Trombe wall

(2) When the fan runs at high speed and the instantaneous value of the total solar radiation reaches 0~1108 W/m^2, the air interlayer of the heat recovery type of heat storage wall can provide a high-quality low-temperature air heat source with the largest temperature difference of 11.89°C between the inlet and outlet air. This part of the interlayer air with a higher temperature than the outdoor air can become a high-quality low-temperature air heat source of passive technology (air source heat pump), so as to greatly improve the energy efficiency of air source heat pump

(3) The heat recovery type of heat storage wall can achieve a 13% to 20% utilization rate of solar energy without relying on photovoltaic and photothermal equipment, and the maximum rate can reach 36%. The combined use of solar energy and air source heat pump will further improve the overall energy efficiency of the system

(4) Relying on the analysis on the heat transfer process regarding the heat recovery type of heat storage wall, strategies are put forward for improving the solar energy utilization rate: materials with high transmittance and low reflectivity are used for the light-transmitting part and materials with high absorptivity are used for the heavy outer wall surface. In the following research, the system will be further optimized according to these strategies

Data Availability

The data used to support the findings of this study are available from the corresponding author upon request.

Conflicts of Interest

No potential conflict of interest was reported by the authors.

References

[1] H. Brandl, "Energy piles for heating and cooling of buildings," in *Proceedings of 7th International Conference&Exhibition on Pilling and Deep Foundations*, pp. 341–346, Vienna, Austria, 1998.

[2] M. M. Yuan, G. M. Chu, T. Yu, Y. Sun, and X. N. Qu, "Summer condition operation test and performance analysis of a hotel GSHP system," *Building Energy & Environment*, vol. 32, no. 3, pp. 33–36, 2013.

[3] H. Brandl, "Energy foundations and other thermo-active ground structures," *Geotechnique*, vol. 56, no. 2, pp. 81–122, 2006.

[4] D. Adam and R. Markiewicz, "Energy from earth-coupled structures, foundations, tunnels and sewers," *Geotechnique*, vol. 59, no. 3, pp. 229–236, 2009.

[5] M. Rabani and V. Kalantar, "Numerical investigation of the heating performance of normal and new designed Trombe wall," *Heat and Mass Transfer*, vol. 52, pp. 1139–1151, 2015.

[6] C. Chen, Y. F. Liu, D. J. Wang, and J. P. Liu, "The optimization and adaptation analysis on the insulation structure of the Trombe wall," *Acta Energiae Solaris Sinica*, vol. 37, no. 11, pp. 2889–2895, 2016.

[7] R. Elghamry and H. Hassan, "Experimental investigation of building heating and ventilation by using Trombe wall coupled with renewable energy system under semi-arid climate conditions," *Solar Energy*, vol. 201, pp. 63–74, 2020.

[8] T. C. Shen, *Study on Heat Distribution and Design Strategy of the Room Heated by Trombe Wall*, Xi'an University of Architecture and Technology, 2019.

[9] Y. Liu, X. Chen, and X. Y. Wang, "Heat transfer model and mathematics simulation of Trombe wall to cavity construction system," *Journal of Xi'an University of Architecture & Technology*, vol. 50, no. 6, pp. 890–894, 2018.

[10] M. Rabani and M. Rabani, "Heating performance enhancement of a new design Trombe wall using rectangular thermal fin arrays: an experimental approach," *Journal of Energy Storage*, vol. 24, article 100796, 2019.

[11] X. Y. Sun and X. Wang, "Optimization of the heating performance of phase-change Trombe wall ——Lhasa as an example," *Building Science*, vol. 35, no. 4, pp. 36–42, 2019.

[12] L. Q. Lou, L. Yan, L. Tang, Y. Liu, Y. P. Feng, and Q. L. Gao, "Dynamic heat preservation at night for a Trombe wall with a built-in panel curtain in Western China," *Solar Energy*, vol. 213, pp. 284–299, 2021.

[13] D. Li, P. Lin, and Y. M. Chen, "Study and analysis of air flow characteristics in Trombe wall," *Renewable Energy*, vol. 162, pp. 234–241, 2020.

[14] J. V. Anderson, J. W. Mitchell, and W. A. Beckman, "A design method for parallel solar-heat pump systems," *Solar Energy*, vol. 25, no. 2, pp. 155–163, 1980.

[15] Z. Liu, Y. Liu, D. Wu, G. Jin, H. Yu, and W. Ma, "Performance and feasibility study of solar-air source pump systems for low-energy residential buildings in alpine regions," *Journal of Cleaner Production*, vol. 256, p. article 120735, 2020.

[16] T. H. Long, Z. Y. Qiao, M. L. Wang et al., "Performance analysis and optimization of a solar-air source heat pump heating system in Tibet, China," *Energy and Buildings*, vol. 220, article 110084, 2020.

[17] G. Panaras, E. Mathioulakis, and V. Belessiotis, "Investigation of the performance of a combined solar thermal heat pump hot water system," *Solar Energy*, vol. 93, pp. 169–182, 2013.

[18] C. J. Banister and M. R. Collins, "Development and performance of a dual tank solar-assisted heat pump system," *Applied Energy*, vol. 149, pp. 125–132, 2015.

[19] O. Kara, K. Ulgen, and A. Hepbasli, "Exergetic assessment of direct-expansion solar-assisted heat pump systems: review and modeling," *Renewable and Sustainable Energy Reviews*, vol. 12, no. 5, pp. 1383–1401, 2008.

[20] Y. Liu, J. Ma, G. Zhou, C. Zhang, and W. Wan, "Performance of a solar air composite heat source heat pump system," *Renewable Energy*, vol. 87, pp. 1053–1058, 2015.

[21] W. Huang, J. Ji, N. Xu, and G. Li, "Frosting characteristics and heating performance of a direct-expansion solar- assisted heat pump for space heating under frosting conditions," *Applied Energy*, vol. 171, pp. 656–666, 2016.

[22] B. Wang, *Trombe Wall Heat Transfer Process and Optimization Design Research*, Xi'an University of Architecture and Technology, 2012.

[23] D. Sun and L. Wang, "Research on heat transfer performance of passive solar collector-storage wall system with phase change materials," *Energy and Buildings*, vol. 119, pp. 183–188, 2016.

[24] J. Long, M. Jiang, J. Lu, and A. Du, "Vertical temperature distribution characteristics and adjustment methods of a Trombe wall," *Building and Environment*, vol. 165, article 106386, 2019.

[25] I. Hernandez-Lopez, J. Xaman, Y. Chavez, I. Hernandez-Perez, and R. Alvarado-Juarez, "Thermal energy storage and losses in a room-Trombe wall system located in Mexico," *Energy*, vol. 109, pp. 512–524, 2016.

[26] S. Y. Wu, L. Xu, and L. Xiao, "Performance study of a novel multi-functional Trombe wall with air purification, photovoltaic, heating and ventilation," *Energy Conversion and Management*, vol. 203, p. 112229, 2020.

[27] M. Z. Pan, Y. F. Liu, Y. Zhou, and S. G. Tian, "Simplified calculation method for heat transfer of Tromble wall," *Journal of Xi'an University of Architecture & Technology*, vol. 52, no. 4, pp. 594–601, 2020.

[28] J. Ji, H. Yi, W. He, G. Pei, J. P. Lu, and B. Jiang, "Numerical study on the photo-thermal and electrical performance of a novel Trombe wall with PV cells," *Acta Energiae Solaris Sinica*, vol. 27, no. 9, pp. 870–877, 2006.

[29] J. Long, A. Yongga, and H. Sun, "Thermal insulation performance of a Trombe wall combined with collector and reflection layer in hot summer and cold winter zone," *Energy and Buildings*, vol. 171, pp. 144–154, 2018.

[30] S. P. Duan, C. J. Jing, and Z. Q. Zhao, "Energy and exergy analysis of different Trombe walls," *Energy and Buildings*, vol. 126, pp. 517–523, 2016.